

Article

Novel Hydroxyl-Containing Quaternary Ammonium Salt N-(2-Hydroxyethyl)-N, N-Dimethyl-3-[(1-Oxododecyl)amino]-1-Propanaminium: Its Synthesis and Flotation Performance to Quartz

Benying Wang ¹, Panxing Zhao ^{2,*}, Wengang Liu ^{2,*} , Wenbao Liu ^{2,3} , Ying Guo ², Kelin Tong ² and Xudong Chen ²

¹ College of Environmental and Safety Engineering, Shenyang University of Chemical Technology, Shenyang 110142, China; wangbenying@syuct.edu.cn

² School of Resources and Civil Engineering, Northeastern University, Shenyang 110819, China; liuwenbao@mail.neu.edu.cn (W.L.)

³ Guizhou Academy of Sciences, Guiyang 550001, China

* Correspondence: 2010416@stu.neu.edu.cn (P.Z.); liuwengang@mail.neu.edu.cn (W.L.)

Abstract: In this paper, a novel hydroxyl-containing quaternary ammonium surfactant N-(2-Hydroxyethyl)-N, N-dimethyl-3-[(1-oxododecyl)amino]-1-propanaminium (LPDC) was synthesized and introduced as a collector for the reverse cationic flotation separation of apatite from quartz; the adsorption mechanisms between LPDC and two mineral surfaces were investigated by Fourier transform infrared spectrometer (FTIR), zeta potential measurements and X-ray photoelectron spectroscopy (XPS) analysis. The micro-flotation tests showed that LPDC exhibited excellent flotation performance. When the pulp was at natural pH and LPDC concentration was 25 mg/L, the apatite concentrate with a P₂O₅ recovery of 95.45% and P₂O₅ grade of 38.94% could be obtained from artificially mixed minerals. FTIR, zeta potential, and XPS analysis indicated that the adsorption of LPDC onto quartz surface is stronger than that onto apatite surface; meanwhile, the adsorption of LPDC onto quartz surface is mainly provided by electrostatic force and hydrogen bonding.

Keywords: synthesis; flotation; quartz; apatite; cationic collector



Citation: Wang, B.; Zhao, P.; Liu, W.; Liu, W.; Guo, Y.; Tong, K.; Chen, X. Novel Hydroxyl-Containing Quaternary Ammonium Salt N-(2-Hydroxyethyl)-N, N-Dimethyl-3-[(1-Oxododecyl)amino]-1-Propanaminium: Its Synthesis and Flotation Performance to Quartz. *Minerals* **2023**, *13*, 702. <https://doi.org/10.3390/min13050702>

Academic Editor: Chiharu Tokoro

Received: 14 April 2023

Revised: 8 May 2023

Accepted: 15 May 2023

Published: 21 May 2023



Copyright: © 2023 by the authors. Licensee MDPI, Basel, Switzerland. This article is an open access article distributed under the terms and conditions of the Creative Commons Attribution (CC BY) license (<https://creativecommons.org/licenses/by/4.0/>).

1. Introduction

Phosphorus plays an indispensable role in the growth and development of plants, and is involved in the composition and metabolism of plants [1,2]. Soil is the main source of phosphorus for plants. As the world population grows and the desire for food production becomes urgent, there is the need to apply phosphorus fertilizer to the soil and the demand for it is increasing. [3]. Phosphate ore is one of the raw materials for the production of phosphate fertilizer [4]. However, most of the phosphate deposits in China are low-grade apatite associated with quartz, mica, clay minerals, and other gangue minerals, which are therefore difficult to be utilized directly [5,6]. So, purifying the low-grade phosphate ores is necessary to satisfy the demand for high-grade raw materials.

Flotation is one of the important technologies used for separation and purification by utilizing the differences in wettability of mineral surfaces [7–9]. The floatability of natural minerals is not sufficient to separate apatite from quartz; thus, it is essential to add flotation reagents to widen the difference in floatability [10–13]. To achieve the separation of apatite from silica-bearing minerals, anionic (fatty acid-based) collectors are usually used to collect apatite directly [14,15]. Unfortunately, their disadvantages, such as intolerance of low temperature and water hardness, have limited their application [16,17]. Therefore, cationic reverse flotation technology is gradually being applied to the apatite desilication process [18–20].

In the initial stages, primary amines ($R-NH_2$) were used for flotation desilication [21]. For example, dodecyl amine (DDA) was commonly used as a cationic collector due to its low cost and easy access [22,23]. However, DDA as a collector suffers from poor solubility and low selectivity, which has limited its promotion and application [24–26]. To overcome these drawbacks, researchers have introduced amines with reactive groups, such as ether amines ($-O-$), amides ($-CONH-$), polyamines ($R_1-NH-R_2-NH_2$), and quaternary ammonium salts ($R-NH_3^+$), to synthesize a series of novel reagents as collectors for mineral reverse flotation desilication process. Researchers such as Zhu et al. have studied the flotation performance of alkyl diamine ether (GE-609) on quartz and investigated the flotation mechanism [27]. Zhao et al. studied the flotation ability of an amide-type surfactant, dimethylaminopropyl lauramide (DPLA), on quartz when it was used as the collector, and analyzed the adsorption mechanism [28]. Liu et al. synthesized a novel collector N-dodecylethylenediamine (ND) and proved that ND has an excellent flotation effect on quartz [29]. Sun et al. used N-hexadecyltrimethylammonium chloride (HTAC) as the collector to efficiently separate magnesite from quartz [30]. Liu et al. synthesized the hydroxyl-group-containing ($-OH$) surfactants N-dodecyl-isopropanolamine (NDIA) and bis(2-hydroxyethyl)dodecylamine (BHDA), and investigated their collector abilities on quartz [31,32]. From the above literature, it can be summarized that quaternary amine collectors have better solubility and flotation performances compared to other amine collectors; meanwhile, the introduction of an O atom could add to the active sites of the collector and enhance hydrogen bonding, leading to improved selectivity. So, these conclusions could give provide direction and inspiration for the design of collectors.

In this study, N-(2-Hydroxyethyl)-N, N-dimethyl-3-[(1-oxododecyl)amino]-1-propylammonium (LPDC) was synthesized in the laboratory and employed as a novel cationic collector in the reverse flotation separation of apatite and quartz. The LPDC structure was characterized by Fourier transform infrared spectrometry (FTIR), 1H nuclear magnetic resonance spectroscopy (1HNMR) and mass spectrometry (MS). The LPDC flotation performance was investigated by micro-flotation tests, and the adsorption mechanisms were analyzed by FTIR, zeta-potential measurements, and XPS.

2. Materials and Methods

2.1. Minerals

The apatite and quartz mineral samples used in this study were obtained from Guizhou province and Liaoning province, P.R. China, respectively. Firstly, the large mineral blocks were smashed to about -5 mm by using a gauze-wrapped hammer (to avoid iron contamination). The high-grade mineral fractions were carefully selected by hand and then placed in a ceramic ball mill for grinding. Finally, a standard sieve was used to obtain the particle size of $-74 + 38 \mu m$ for flotation and other analyses [33]. The quartz and apatite samples that met the particle size range were further purified by the hydrochloric acid leaching method and shaking table method, respectively [16,18]. The mineral composition of the two mineral samples were analyzed by X-ray diffraction spectra (XRD), and the results are given in Figure 1. In addition, the chemical analysis of P_2O_5 in apatite and SiO_2 in quartz were carried out and the results were 39.94% and 99.42%, respectively, which were used as the feed samples for flotation tests and other analyses.

2.2. Reagents

A two-step synthesis of LPDC was carried out in the laboratory; the synthesized routes are shown in Scheme 1. Firstly, a three-necked flask containing 0.10 mol lauric acid, 20 mL toluene, and a magnetic stirrer was placed in an oil bath. The system was heated to $100^\circ C$ to ensure the lauric acid had completely dissolved. Then, the 0.15 mol 3-(Dimethylamino)-1-propylamine was added dropwise slowly to the three-necked flask through a pressure-equalizing funnel (approximately 3 h for dropwise completion). After that, continued to be heated at $140^\circ C$ and reacted for 12 h. With the reaction complete, the toluene and excess 3-(Dimethylamino)-1-propylamine were evaporated under reduced pressure. The crude

product was recrystallized by petroleum ether 2 times, followed by drying in a vacuum oven for 24 h to obtain the target product of the first step—(Laurylamidopropyl)dimethylamine (DPLA).

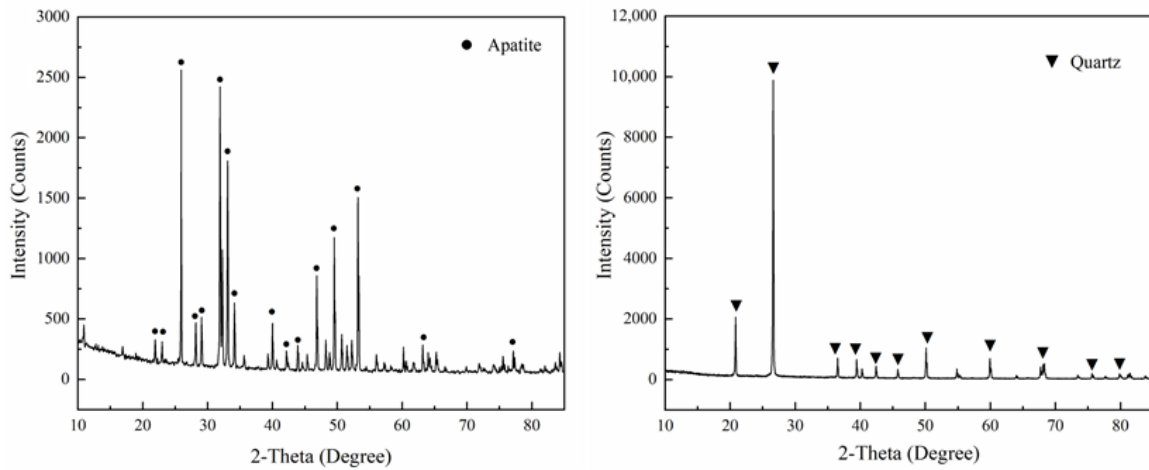
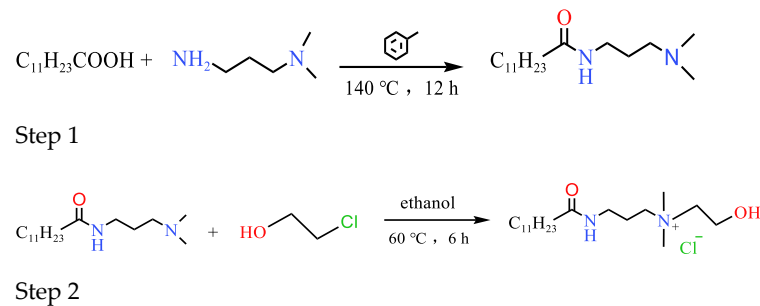


Figure 1. XRD patterns of apatite and quartz.



Scheme 1. The synthesis procedure of LPDC.

The purified (Laurylamidopropyl)dimethylamine was placed in a three-neck flask, the system was heated to 60 °C, and then 2-chloroethanol was slowly added dropwise into the system through a constant-pressure dropping funnel (2 h dropwise completion), and the reaction was continued at 60 °C for 12 h. Following completion of the reaction, the solvent and unreacted materials were removed by distillation under reduced pressure to obtain the crude product of LPDC. Finally, the unpurified product was recrystallized 5 times by acetone to obtain the LPDC concentrated product.

Sodium hydroxide (NaOH) and hydrochloric acid (HCl) were used to adjust the pulp pH, which was provided by Sinopharm Chemical Reagent Co., Ltd., Shanghai, China. All the reagents were of analytical grade purity. Deionized water was used in all the tests to avoid the influence of water quality on the experiments.

2.3. Flotation Tests

The micro-flotation tests of single minerals and artificial mixed minerals were conducted at an XFG_{II}-5 laboratory flotation machine (Jilin Exploration Machinery Plant, Changchun, China) with a 40 mL flotation cell; the impeller spindle speed was 1992 r/min. The flotation process is shown in Figure 2. A mass of 2 g single mineral sample or artificially mixed minerals samples (the mass ratio of apatite: quartz was 3:2) and 30 mL deionized water were placed into the flotation cell, then the pulp pH was adjusted to a predetermined pH (if required) and conditioned for 2 min, followed by addition of the collector, and again conditioned for 2 min before flotation. The flotation scraping time was 4 min, and the concentrates and tailings were separately filtered, dried, and weighted, and the grade of P₂O₅ in concentrates was assayed.

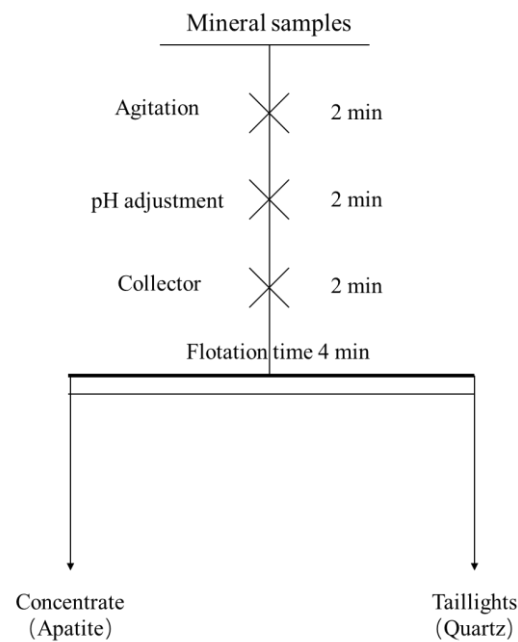


Figure 2. Flowsheet of flotation tests.

The yields were taken as the single mineral flotation tests recoveries. For the artificially mixed mineral flotation, the recovery was calculated by Equation (1) [34]:

$$\varepsilon = \frac{\gamma\beta}{\alpha} \quad (1)$$

where ε and β are the recovery and grade of P_2O_5 in concentrate, respectively; γ is the yield of concentrate; and α is the P_2O_5 grade of the feed. Each test was repeated three times and the average value was taken as the final result.

2.4. FTIR Measurements

A Thermo Scientific Nicolet 380 FTIR spectrometer (Thermo Fisher Scientific Inc., Waltham, MA, USA) was employed to record the FTIR data of LPDC, the pure minerals, the and minerals treated with LDPC. All the measurements were conducted in a dry and room-temperature (25 ± 2 °C) environment. Prior to testing, the quartz or apatite samples were ground to below $5 \mu\text{m}$ by an agate mortar and the finely ground mineral samples were added to deionized water without and with 25 mg/L LDPC; the powder was stirred for 30 min by a magnetic stirrer and then filtered, and dried at low temperature in a vacuum drying oven (40 ± 2 °C) for 24 h [35]. Then, 5 mg of dry samples were mixed with 0.5 g KBr (mass ratio of samples: KBr = 1:100) and the test specimens were prepared according to the KBr pellet method, with a wavenumber range of $400\text{--}4000 \text{ cm}^{-1}$.

2.5. Zeta Potential Determinations

The zeta potential measurements of apatite and quartz before or after treatment with LPDC were performed on a Nano-ZS90 zeta potential analyzer (Malvern Instruments Ltd., Malvern, UK). In each test, 20 mg finely ground ($-5 \mu\text{m}$) minerals and 30 mL deionized water or 25 mg/L LDPC solution were placed in a 50 mL baker, using NaOH and HCl solution to adjust the slurry to the predetermined pH. Then, the slurry was agitated by magnetic stirring equipment for 10 min and allowed to stand for 5 min [36]. The supernatant was filled into the electrolyzer and the measurements were taken as required by the instrument. The results applied in this study were the average value of five independent measurements.

2.6. XPS Measurements

A Thermo Scientific K-Alpha with Al X-ray (1486.6 eV) as the sputtering source was used to conduct the XPS measurements. The Thermo Scientific Advantage v5.52 was used to analyze XPS spectra. The peak of C 1s spectrum with a bounding energy of 248.8 eV was used as the calibrating binding energy. The preparation of samples for XPS measurements was the same as that of the FTIR measurements.

3. Results and Discussions

3.1. Characterization of LPDC

FTIR, ^1H NMR and MS were used to characterize the structure of LPDC. The FTIR spectrum of LPDC is shown in Figure 3. It can be seen that the characteristic peaks at 3294 cm^{-1} and 3177 cm^{-1} were the stretching vibration of N-H in NH_4^+ [37]. The peaks at 2916 cm^{-1} , 2849 cm^{-1} , 1463 cm^{-1} , 1348 cm^{-1} and 719 cm^{-1} were referred to the asymmetrical stretching vibration, symmetric stretching vibration, bending vibration, in-of-plane wagging vibration and out-of-plane wagging vibration of $-\text{CH}_2-$, respectively. The peaks at 1637 cm^{-1} and 1552 cm^{-1} were attributed to the stretching vibration of C=O and the C-N-H bending vibration, respectively [38,39]. The peak at 1124 cm^{-1} was referred to the stretching vibration of C-C. The peak at 1048 cm^{-1} was referred to the stretching vibration of C-OH. The ^1H NMR spectrum analysis of LPDC indicated that ^1H NMR (400 MHz, CDCl_3): δ ppm 5.59 (s, 1H, NH(CONH)), δ 4.03 (s, 1H NHR_2^+), δ 3.59 (dt, $J = 11.4, 4.9\text{ Hz}$, 6H, 3 CH_2), δ 3.25 ppm (s, 6H, 2 CH_3), δ 2.20 ppm (q, $J = 8.0\text{ Hz}$, 2H CH_2), δ 2.10–1.49 ppm (m, 4H, 2 CH_2), δ 1.24 ppm (d, $J = 7.6\text{ Hz}$, 18H, 9 CH_2), and δ 0.86 ppm (t, $J = 6.6\text{ Hz}$, 3H, CH_3). The MS (ESI $^+$): calculated for $\text{C}_{19}\text{H}_{41}\text{N}_2\text{O}_2^+$ 328.48; found 329.13 [M+H]. The characterization showed that the synthesized product was the target product.

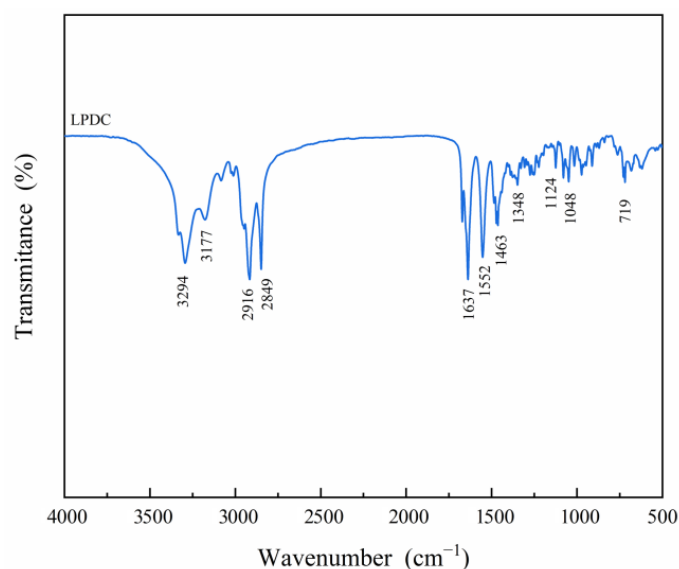


Figure 3. The FTIR of LPDC molecules.

3.2. Flotation Tests of Single Minerals

The collecting ability of the novel collector could be evaluated by single mineral flotation tests; therefore, the flotation tests were carried out and the curves of the flotation recovery are shown in Figures 4 and 5.

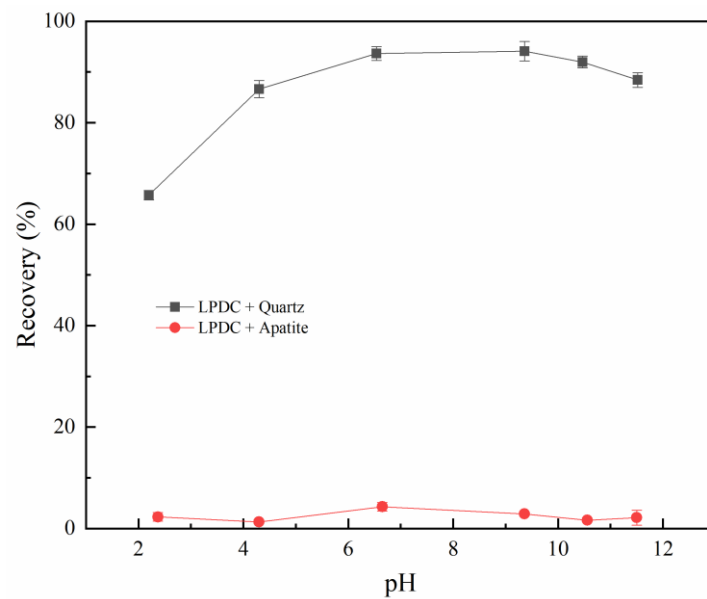


Figure 4. Effect of pulp pH on the flotation behaviors of apatite and quartz with 20 mg/L collector.

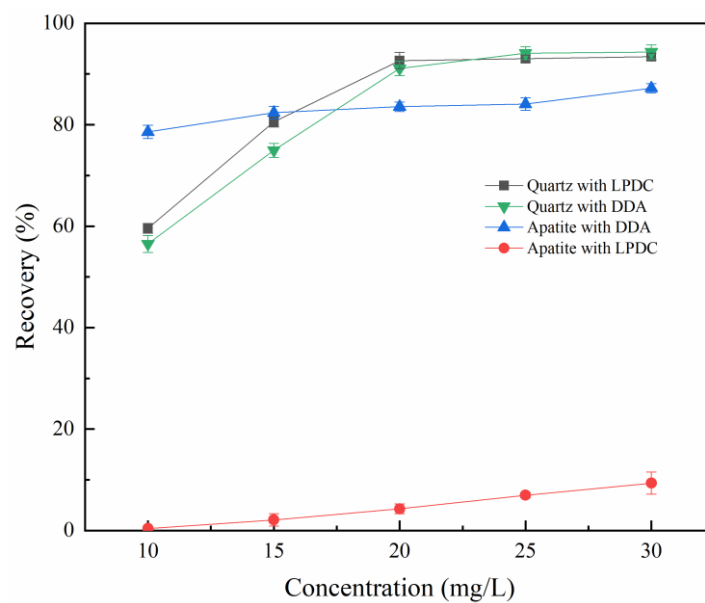


Figure 5. Effect of LPDC and DDA concentration on the flotation behaviors of quartz and apatite at natural pulp pH.

Figure 4 shows the flotation behaviors of quartz and apatite as the function of pulp pH when the collector LPDC was at 20 mg/L. It is clearly illustrated by the flotation results in Figure 4 that the recovery of quartz is much higher than that of apatite in the pulp pH range of 2–12. So the effect of pulp pH on the foam recovery of quartz is significantly greater than that of apatite. The recovery of quartz increased with the pulp pH when it was below the natural pulp pH (6.5), and reached a maximum recovery of 92.70% at the natural pulp pH. However, the quartz recovery decreased slightly when the pulp pH continued to increase, and always remained above 90%, whereas for apatite, recovery fluctuated slightly with changes in pulp pH; its recovery was always below 10% at the tested pulp pH range, and reached a maximum recovery of 6.30% at the natural pulp pH (6.6). From the above research, it can be conducted that the alkaline pulp environment is favorable for the separation of quartz and apatite when LPDC is used as collector. To assess the collecting performance of LPDC, the conventional cationic collector DDA was introduced

as a reference. The effects of the LPDC and DDA concentrations on the recoveries of quartz and apatite at the natural pulp pH are shown in Figure 5. It can be noted that both quartz and apatite recoveries increased with increasing concentration of both LPDC and DDA from 10 mg/L to 25 mg/L. When the concentration was at 25 mg/L, the collection capacity of the two collectors for quartz seemed to be at a maximum, and at this point, the recoveries of quartz were 93.05% (LPDC) and 94.12% (DDA), respectively. There were no significant changes in the quartz recoveries when the concentration of both collectors continued to increase. However, it can be concluded that the recovery of apatite is closely related to the type of collector. Although the apatite recoveries both increased slowly with the increase in concentration of the two collectors, the difference in the recovery was obvious. When DDA was used as a collector, the apatite recovery increased from 78.58% to 87.20% when the collector concentration increased from 10 mg/L to 30 mg/L. While the LPDC was used as the collector, the apatite recoveries were always below 10% in the tested concentration range. Therefore, it can be concluded from the recoveries of both minerals that LPDC has better selectivity than DDA.

3.3. Flotation Tests of Artificial Minerals

Based on the single mineral flotation, artificially mixed mineral flotation tests were carried out to further assess the separation performance of LPDC on apatite and quartz. The results are shown in Figures 6 and 7.

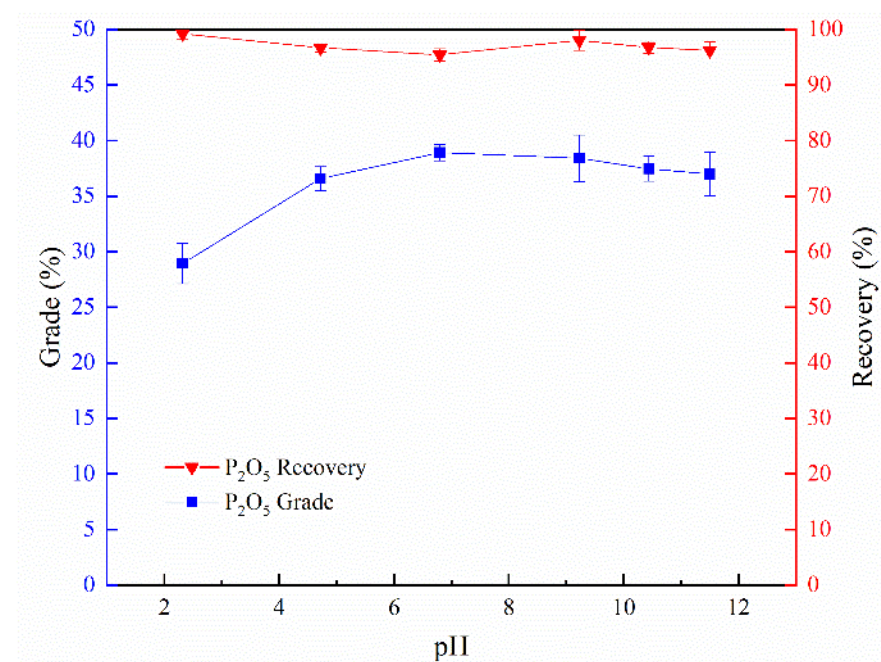


Figure 6. Effect of pulp pH on the flotation of artificially mixed minerals (LPDC 25 mg/L).

Figure 6 shows the effect of pulp pH on the flotation of artificially mixed minerals with 25 mg/L LPDC. Since the apatite desilication process was a reverse flotation process, the apatite concentrate was left in the flotation cell. It can be seen that with the increase in pulp pH, the grade of apatite concentrate showed a trend of first decreasing and then slightly decreasing; however, its recovery always remained at a high level. At the natural pulp pH, the apatite concentrate reached a maximum grade of 38.94% (the P₂O₅ grade of the apatite sample was 39.94%) and the recovery was 95.45%. This indicated that the LPDC has excellent separation efficiency on quartz and apatite under natural pulp pH.

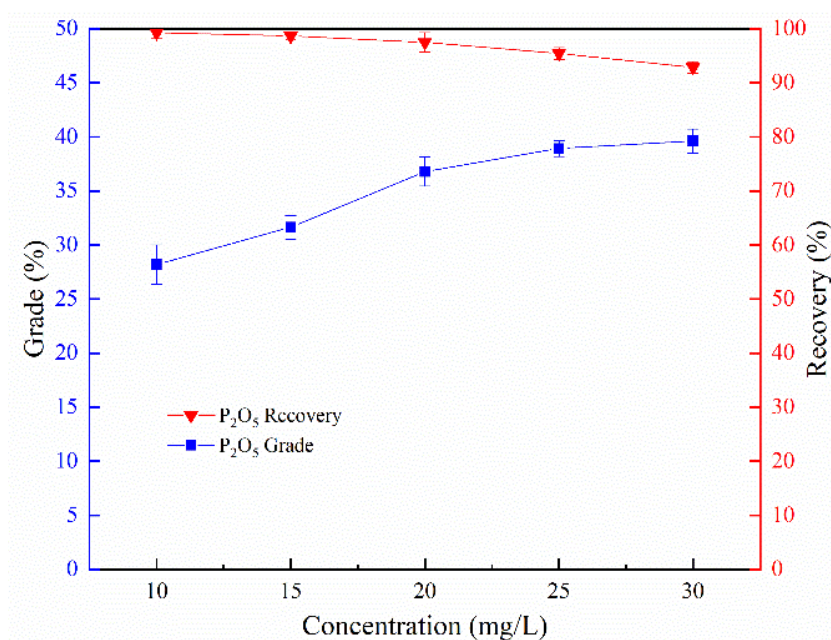


Figure 7. Effect of LPDC concentration on the flotation of artificially mixed minerals at natural pulp pH.

The effects of LPDC concentration on the flotation of artificially mixed minerals of quartz and apatite at the natural pulp pH were investigated; the results are displayed in Figure 7. It can be seen from Figure 7 that at an LPDC concentration from 10 mg/L to 30 mg/L, the recovery of apatite gradually decreased while its grade gradually increased, due to some of the apatite being entrained and floated out during the collecting of the quartz. When the LPDC concentration was at 25 mg/L, the apatite recovery reached 95.45%, and the grade of the apatite concentrate was 38.94%. Continuing to increase the LPDC concentration not only decreased the grade of apatite but also decreased its recovery. So, it can be concluded that the optimal concentration of LPDC for separating apatite and quartz artificially mixed mineral is 25 mg/L. The LPDC has the potential to become an effective collector for apatite desilication.

3.4. FTIR Analysis

FTIR can be used to determine the functional groups of substances by their characteristic peaks [40]. The FTIR can not only investigate and analyze the structure of compounds, but also can be used in the field of flotation to analyze and study the adsorption mechanism between flotation reagent and mineral surface. The FTIR spectra of quartz and apatite before and after treatment with LPDC at the natural pulp pH are shown in Figure 8.

The FTIR spectra were resolved according to the standard database and the previous literature. As shown in Figure 8a, in the quartz FTIR spectrum, the peak around 1082 cm^{-1} was due to the asymmetrical stretching vibration of Si-O-Si; the peaks at 778 cm^{-1} and 684 cm^{-1} were the symmetric stretching vibration of Si-O-Si, and the asymmetric bending vibration of Si-O [25,41], respectively. After the reaction of quartz with LPDC, new characteristic peaks could be seen on the FTIR spectrum of quartz. The strong and broad peak around 3439 cm^{-1} corresponded to the characteristic peak of -OH stretching vibration, which was maybe due to the formation of hydrogen bonds between the -OH of LPDC and the quartz surface. The new peaks which appeared at 2924 cm^{-1} and 2853 cm^{-1} were referred to the asymmetrical stretching vibration and the symmetric of -CH₂-, respectively. These results, along with the appearance of the new characteristic peaks in the quartz FTIR curve, could be related to the adsorption process. According to previous studies [41,42], it is assumed that physical adsorption and hydrogen bonding adsorption of LPDC may have occurred on the quartz.

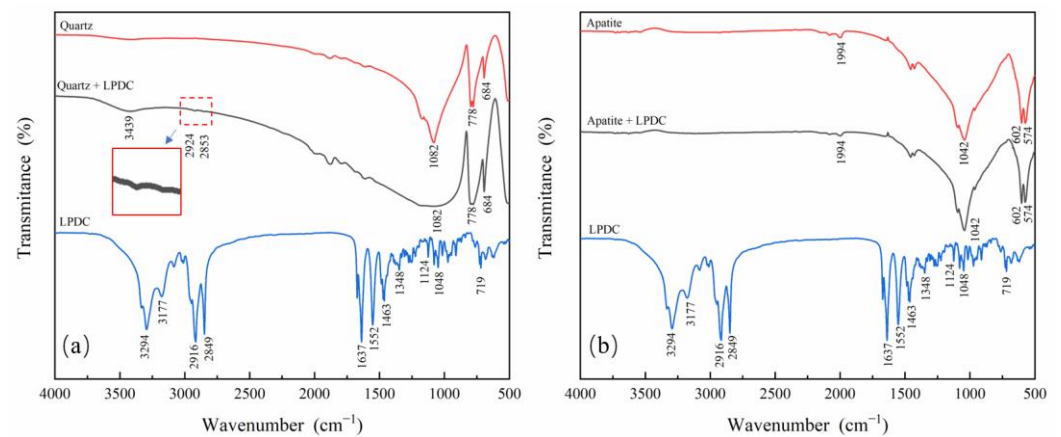


Figure 8. FTIR spectrum of (a) quartz and (b) apatite before and after treatment with LPDC.

For apatite, it can be seen in Figure 8b that the peaks around 1994 cm^{-1} , 1042 cm^{-1} were the asymmetrical stretching vibration of PO_4^{2-} , and the peaks around 602 cm^{-1} and 574 cm^{-1} were the symmetrical stretching vibration of PO_4^{2-} . A comparison of the FTIR spectra of apatite before and after LPDC treatment showed that no new characteristic peaks appeared on the FTIR curve of apatite after LPDC treatment, which indicated that LPDC may not be strongly absorbed on the apatite surface.

3.5. Zeta Potential Measurements

In the case of minerals in contact with water, the transfer of charged electrons will occur at the mineral surface, and cause the mineral surface to be charged [43]. The adsorption of flotation reagents at the solid–liquid interface is often influenced by the electrical properties of the particle surface, so the adsorption mechanism between the flotation reagent and the mineral surface can be investigated according to the changes in the electrical properties in the mineral surface. The zeta potential of quartz and apatite before and after treatment with 25 mg/L LDPC under different pulp pHs are shown in Figure 9.

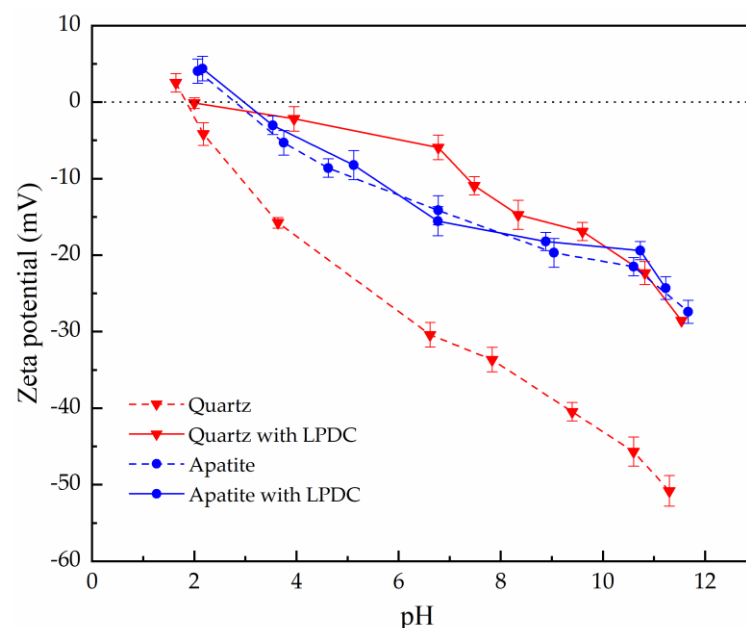


Figure 9. Zeta potential of quartz and apatite as a function of pH (LPDC 25 mg/L).

As can be seen in Figure 9, under the same pulp pH environment, the zeta potentials of quartz are more negative than those of apatite in the test range. The point of zero charges (PZC) of quartz and apatite are 1.9 and 2.9, respectively [15,44], which is in accordance with those previously reported. When the pulp pH increases, the zeta potential of both quartz and apatite gradually decreases. It can be clearly seen that there is a significant shift in the surface potential of quartz to a more negative zeta potential after the LPDC treatment; however, the zeta potential of apatite only fluctuates in a small range and no regular shift occurs. From the results, it can be conducted that the adsorption of LPDC is primarily on the quartz surface.

3.6. XPS Analysis

XPS is an effective tool for detecting the elemental composition, content and chemical state of the mineral surface. The XPS results of quartz before and after treatment with LPDC under the natural-pulp-pH condition are listed in Table 1 and Figures 10 and 11.

Table 1. The atomic concentrations of the main elements on quartz and quartz treated with 25 mg/L LPDC at natural pulp pH.

Sample	Atomic Concentration (%)			
	C 1s	O 1s	N 1s	Si 2p
quartz	18.8	52.6	-	28.6
quartz + LPDC	22.2	49.7	2.9	27.2

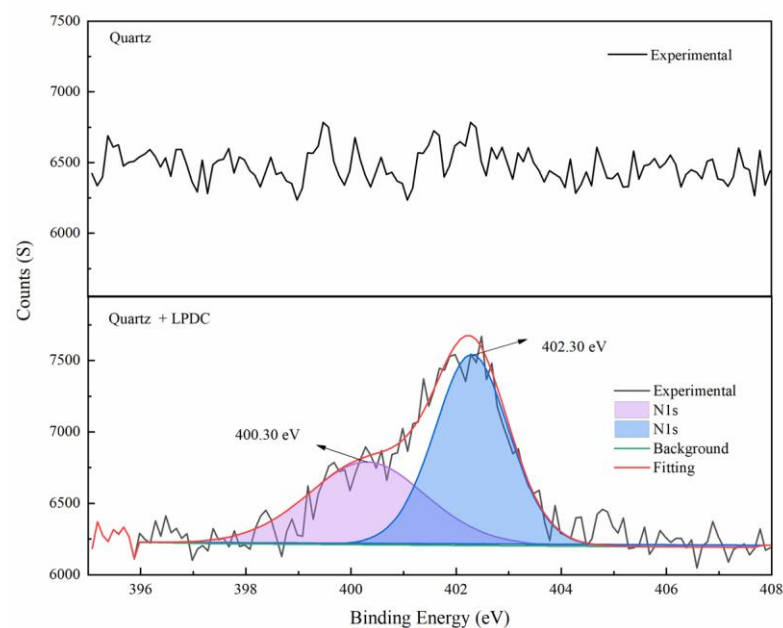


Figure 10. N1s XPS spectra of quartz and quartz treated with LPDC.

From Table 1, it can be seen that pure quartz only contains three elements of C (due to the exposure of the samples to the air, carbon-containing contaminants were formed), O, and Si. After treatment with LPDC, the relative atomic concentration of the representative atoms on the quartz surface changed, where the N element was detected. As can be seen in Figure 10, two N1s signals on the LPDC-treated quartz surface were observed at 402.3 eV and 400.3 eV, which were assigned to N in the first anchored adsorption layer and the higher (second, third, etc.) layers, respectively [45], and indicates that the adsorption of LPDC occurred on the quartz surface.

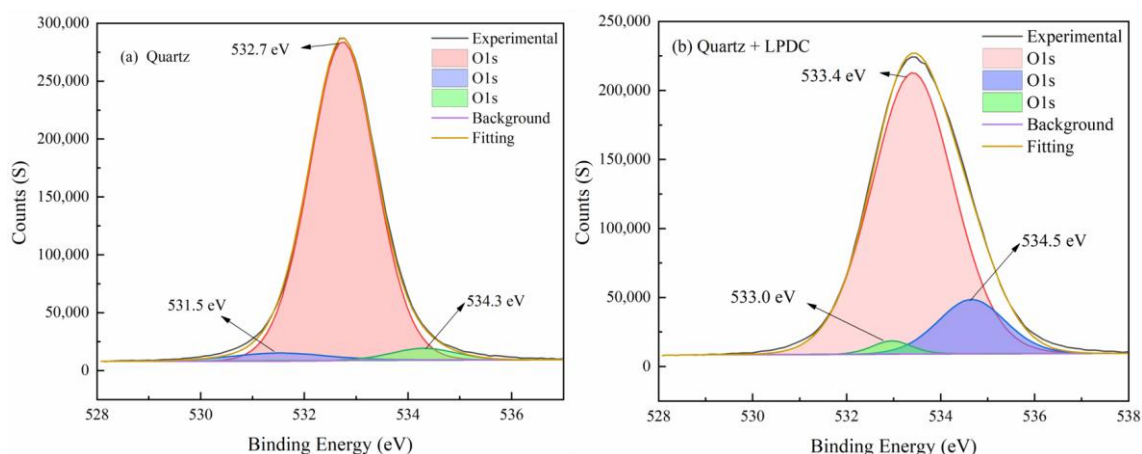


Figure 11. O1s XPS spectra of quartz and quartz treated with LPDC.

From Figure 11, peaks in the binding energy of 531.5 eV, 532.7 eV, and 534.3 eV on the pure quartz surface were detected, which were attributed to the element O in Si-OH, and Si-O-/Si-O-Si, respectively [24,45]. After LPDC treatment, the signals of the binding energy of O1s had been changed to 533.0 eV, 533.4 eV, and 534.5 eV. These shifts indicated that the adsorption of LPDC may have broken the original bonds and formed new hydrogen bonds on the quartz surface. The negatively charged Si-O- on the quartz surface could be combined with RNH_4^+ of LPDC in the solution by electrostatic attraction. Furthermore, the binding energy shifts of O1s are also affected by the hydrogen bond (Si-OH ... N-R, Si-O ... HO-R) [34,46]. The XPS results were agreement with the results of the analysis obtained by FTIR and zeta potential.

4. Conclusions

To overcome the challenge of poor solubility for conventional cationic collectors, a novel hydroxyl-containing quaternary ammonium salt, N-(2-Hydroxyethyl)-N,N-dimethyl-3-[(1-oxododecyl)amino]-1-propanaminium (LPDC), was synthesized and characterized, then it was introduced into the apatite reverse flotation desilication system as the collector. The mechanism of adsorption was studied by FTIR, zeta potential analyses, and XPS.

The FTIR ^1H NMR and MS spectra confirmed that the molecular structure and satisfactory purity of the synthesized product was achieved. The single mineral flotation tests showed that LPDC has a better collecting ability for quartz than that of apatite, and exhibits significant flotation differences. At the natural pulp pH and an LPDC concentration of 25 mg/L, an apatite concentrate with a P_2O_5 grade of 38.94% and recovery of 95.45% was obtained from the artificially mixed minerals, which indicated the excellent separation performance of LPDC. FTIR, zeta potential and XPS analyses demonstrated the adsorption of LPDC on the quartz surface was mainly due to physical adsorption, especially electrostatic force and hydrogen bonding.

Author Contributions: B.W.: Investigation, data curation, methodology, formal analysis, writing—original draft; P.Z.: writing—review and editing; W.L. (Wengang Liu): conceptualization, project administration, funding, writing—review and editing; W.L. (Wenbao Liu): investigation, methodology, supervision, writing—review and editing; Y.G.: investigation, methodology, experiment; K.T. and X.C.: supervision, review and editing. All authors have read and agreed to the published version of the manuscript.

Funding: This work was supported by the National Natural Science Foundation of China (grant No. 52104250, 52274254) and the China Postdoctoral Science Foundation (2022M720927).

Data Availability Statement: Not applicable.

Conflicts of Interest: The authors declare no conflict of interest.

References

1. Wesana, J.; De Steur, H.; Dora, M.K.; Mutenyo, E.; Muyama, L.; Gellynck, X. Towards Nutrition Sensitive Agriculture. Actor Readiness to Reduce Food and Nutrient Losses or Wastes along the Dairy Value Chain in Uganda. *J. Clean. Prod.* **2018**, *182*, 46–56. [[CrossRef](#)]
2. Huang, Z.; Cheng, C.; Liu, Z.; Zeng, H.; Feng, B.; Zhong, H.; Luo, W.; Hu, Y.; Guo, Z.; He, G.; et al. Utilization of a New Gemini Surfactant as the Collector for the Reverse Froth Flotation of Phosphate Ore in Sustainable Production of Phosphate Fertilizer. *J. Clean. Prod.* **2019**, *221*, 108–112. [[CrossRef](#)]
3. Han, Y.; Han, S.; Kim, B.; Yang, J.; Choi, J.; Kim, K.; You, K.-S.; Kim, H. Flotation Separation of Quartz from Apatite and Surface Forces in Bubble–Particle Interactions: Role of PH and Cationic Amine Collector Contents. *J. Ind. Eng. Chem.* **2019**, *70*, 107–115. [[CrossRef](#)]
4. Merma, A.G.; Torem, M.L.; Morán, J.J.V.; Monte, M.B.M. On the Fundamental Aspects of Apatite and Quartz Flotation Using a Gram Positive Strain as a Bioreagent. *Miner. Eng.* **2013**, *48*, 61–67. [[CrossRef](#)]
5. Cao, S.; Yin, W.; Yang, B.; Zhu, Z.; Sun, H.; Sheng, Q.; Chen, K. Insights into the Influence of Temperature on the Adsorption Behavior of Sodium Oleate and Its Response to Flotation of Quartz. *Int. J. Min. Sci. Technol.* **2022**, *32*, 399–409. [[CrossRef](#)]
6. Shuai, S.; Huang, Z.; Burov, V.E.; Poilov, V.Z.; Li, F.; Wang, H.; Liu, R.; Zhang, S.; Cheng, C.; Li, W.; et al. Flotation Separation of Wolframite from Calcite Using a New Trisiloxane Surfactant as Collector. *Int. J. Min. Sci. Technol.* **2023**, *33*, 379–387. [[CrossRef](#)]
7. Lei, D.; Gui, W.; Zhao, X.; Tian, X.; Xiao, W.; Xue, J.; Wang, Y.; Peng, X. New Insight into Poor Flotation Recovery of Fine Molybdenite: An Overlooked Phase Transition from 2H to 1T MoS₂. *Sep. Purif. Technol.* **2023**, *304*, 122286. [[CrossRef](#)]
8. Shen, Z.; Tao, J.; Wen, S.; Wang, H.; Zhang, Q.; Feng, Q. Surface Characteristics and Flotation Performance of Quartz in the Presence of Dissolved Components of Malachite. *Colloids Surf. A Physicochem. Eng. Asp.* **2023**, *656*, 130497. [[CrossRef](#)]
9. Sun, W.; Liu, W.; Liu, W.; Li, P.; Chen, X.; Tong, K.; Kou, W. Adsorption Study of Potential Collector Polyoxyethylene Ether Phosphate on Magnesite. *Colloids Surf. A Physicochem. Eng. Asp.* **2023**, *666*, 131282. [[CrossRef](#)]
10. Liu, G.; Yang, X.; Zhong, H. Molecular Design of Flotation Collectors: A Recent Progress. *Adv. Colloid Interface Sci.* **2017**, *246*, 181–195. [[CrossRef](#)]
11. Albijanic, B.; Ozdemir, O.; Nguyen, A.V.; Bradshaw, D. A Review of Induction and Attachment Times of Wetting Thin Films between Air Bubbles and Particles and Its Relevance in the Separation of Particles by Flotation. *Adv. Colloid Interface Sci.* **2010**, *159*, 1–21. [[CrossRef](#)] [[PubMed](#)]
12. Gharabaghi, M.; Aghazadeh, S. A Review of the Role of Wetting and Spreading Phenomena on the Flotation Practice. *Curr. Opin. Colloid Interface Sci.* **2014**, *19*, 266–282. [[CrossRef](#)]
13. Mao, Y.; Wang, Z.; Liu, W.; Tian, P. Effect of TIPA/TEA Combined Grinding Aid on the Behavior of Quartz Flotation in DDA System. *Powder Technol.* **2022**, *406*, 117570. [[CrossRef](#)]
14. Ammar, M.; El-Halim, S.A.; Sharada, H.; Fadel, M.; Yehia, A. Study on the Interactions of Two Models of Enzymes as Eco-Friendly Depressants in Flotation Separation of Apatite from Hematite. *Appl. Surf. Sci.* **2022**, *601*, 154223. [[CrossRef](#)]
15. Derhy, M.; Taha, Y.; Benzaazoua, M.; El-Bahi, A.; Ait-Khouia, Y.; Hakkou, R. Assessment of the Selective Flotation of Calcite, Apatite and Quartz Using Bio-Based Collectors: Flaxseed, Nigella, and Olive Oils. *Miner. Eng.* **2022**, *182*, 107589. [[CrossRef](#)]
16. Luo, B.; Zhu, Y.; Sun, C.; Li, Y.; Han, Y. Flotation and Adsorption of a New Collector α -Bromodecanoic Acid on Quartz Surface. *Miner. Eng.* **2015**, *77*, 86–92. [[CrossRef](#)]
17. Guo, W.; Zhu, Y.; Han, Y.; Li, Y.; Yuan, S. Flotation Performance and Adsorption Mechanism of a New Collector 2-(Carbamoylamino) Lauric Acid on Quartz Surface. *Miner. Eng.* **2020**, *153*, 106343. [[CrossRef](#)]
18. Peng, X.; Liu, W.; Zhao, Q.; Liu, W.; Tong, K.; Zhao, P. Development and Utilization of a Novel Hydrogen Bonding Enhanced Collector in the Separation of Apatite from Quartz. *Miner. Eng.* **2022**, *180*, 107477. [[CrossRef](#)]
19. Feng, Q.; Wang, M.; Zhang, G.; Zhao, W.; Han, G. Enhanced Adsorption of Sulfide and Xanthate on Smithsonite Surfaces by Lead Activation and Implications for Flotation Intensification. *Sep. Purif. Technol.* **2023**, *307*, 122772. [[CrossRef](#)]
20. Zhao, P.; Liu, W.; Liu, W.; Shen, Y.; Cui, B.; Zhao, Q. Novel Low-Foam Viscous Cationic Collector 2-[2-(Tetradecylamino)Ethoxy]Ethanol: Design, Synthesis, and Flotation Performance Study to Quartz. *Sep. Purif. Technol.* **2023**, *307*, 122633. [[CrossRef](#)]
21. Huang, Z.; Zhong, H.; Wang, S.; Xia, L.; Zou, W.; Liu, G. Investigations on Reverse Cationic Flotation of Iron Ore by Using a Gemini Surfactant: Ethane-1,2-Bis(Dimethyl-Dodecyl-Ammonium Bromide). *Chem. Eng. J.* **2014**, *257*, 218–228. [[CrossRef](#)]
22. Yang, L. Intensification of Interfacial Adsorption of Dodecylamine onto Quartz by Ultrasonic Method. *Sep. Purif. Technol.* **2019**, *9*, 115701. [[CrossRef](#)]
23. Luo, J.; Liu, M.; Xing, Y.; Gui, X.; Li, J. Investigating Agglomeration of Kaolinite Particles in the Presence of Dodecylamine by Force Testing and Molecular Dynamics Simulation. *Colloids Surf. A Physicochem. Eng. Asp.* **2022**, *645*, 128930. [[CrossRef](#)]
24. Liu, W.; Liu, W.; Zhao, Q.; Shen, Y.; Wang, X.; Wang, B.; Peng, X. Design and Flotation Performance of a Novel Hydroxy Polyamine Surfactant Based on Hematite Reverse Flotation Desilication System. *J. Mol. Liq.* **2020**, *301*, 112428. [[CrossRef](#)]
25. Liu, C.; Ni, C.; Yao, J.; Chang, Z.; Wang, Z.; Zeng, G.; Luo, X.; Yang, L.; Ren, Z.; Shao, P.; et al. Hydroxypropyl Amine Surfactant: A Novel Flotation Collector for Efficient Separation of Scheelite from Calcite. *Miner. Eng.* **2021**, *167*, 106898. [[CrossRef](#)]
26. Qiao, X.; Liu, A.; Li, Z.; Fan, J.; Fan, P.; Fan, M. Preparation and Properties of Dodecylamine Microemulsion for the Flotation of Quartz and Magnetite. *Miner. Eng.* **2021**, *164*, 106821. [[CrossRef](#)]
27. Zhu, H.; Qin, W.; Chen, C.; Chai, L.; Li, L.; Liu, S.; Zhang, T. Selective Flotation of Smithsonite, Quartz and Calcite Using Alkyl Diamine Ether as Collector. *Trans. Nonferrous Met. Soc. China* **2018**, *28*, 163–168. [[CrossRef](#)]

28. Zhao, P.; Liu, W.; Liu, W.; Tong, K.; Shen, Y.; Zhao, S.; Zhou, S. Efficient Separation of Magnesite and Quartz Using Eco-Friendly Dimethylaminopropyl Lauramide Experimental and Mechanistic Studies. *Miner. Eng.* **2022**, *188*, 107814. [[CrossRef](#)]
29. Liu, W.; Wei, D.; Wang, B.; Fang, P.; Wang, X.; Cui, B. A New Collector Used for Flotation of Oxide Minerals. *Trans. Nonferrous Met. Soc. China* **2009**, *19*, 1326–1330. [[CrossRef](#)]
30. Sun, H.; Yin, W.; Yang, B.; Chen, K.; Sheng, Q. Efficiently Separating Magnesite from Quartz Using N-Hexadecyltrimethylammonium Chloride as a Collector via Reverse Flotation. *Miner. Eng.* **2021**, *166*, 106899. [[CrossRef](#)]
31. Liu, W.; Wang, X.; Wei, D.; Wang, B. Utilization of Novel Surfactant N-Dodecyl-Isopropanolamine as Collector for Efficient Separation of Quartz from Hematite. *Sep. Purif. Technol.* **2016**, *162*, 188–194. [[CrossRef](#)]
32. Liu, W.; Liu, W.; Wang, B.; Zhao, Q.; Duan, H.; Chen, X. Molecular-Level Insights into the Adsorption of a Hydroxy-Containing Tertiary Amine Collector on the Surface of Magnesite Ore. *Powder Technol.* **2019**, *355*, 700–707. [[CrossRef](#)]
33. Wei, Z.; Zhang, Q.; Wang, X. New Insights on Depressive Mechanism of Citric Acid in the Selective Flotation of Dolomite from Apatite. *Colloids Surf. A Physicochem. Eng. Asp.* **2022**, *653*, 130075. [[CrossRef](#)]
34. Sun, H.; Yin, W.; Yao, J. Study of Selective Enhancement of Surface Hydrophobicity on Magnesite and Quartz by N, N-Dimethyloctadecylamine: Separation Test, Adsorption Mechanism, and Adsorption Model. *Appl. Surf. Sci.* **2022**, *583*, 152482. [[CrossRef](#)]
35. Lima, R.M.F.; Brandao, P.R.G.; Peres, A.E.C. The Infrared Spectra of Amine Collectors Used in the Flotation of Iron Ores. *Miner. Eng.* **2005**, *18*, 267–273. [[CrossRef](#)]
36. Liu, W.; Peng, X.; Liu, W.; Wang, X.; Zhao, Q.; Wang, B. Effect Mechanism of the Iso-Propanol Substituent on Amine Collectors in the Flotation of Quartz and Magnesite. *Powder Technol.* **2020**, *360*, 1117–1125. [[CrossRef](#)]
37. Huang, Z. Reverse Flotation Separation of Quartz from Phosphorite Ore at Low Temperatures by Using an Emerging Gemini Surfactant as the Collector. *Sep. Purif. Technol.* **2020**, *7*, 116923. [[CrossRef](#)]
38. Wang, X.; Liu, W.; Duan, H.; Liu, W.; Shen, Y.; Gu, X.; Qiu, J.; Jia, C. Potential Application of an Eco-Friendly Amine Oxide Collector in Flotation Separation of Quartz from Hematite. *Sep. Purif. Technol.* **2021**, *278*, 119668. [[CrossRef](#)]
39. Guo, W.; Han, Y.; Zhu, Y.; Li, Y.; Tang, Z. Effect of Amide Group on the Flotation Performance of Lauric Acid. *Appl. Surf. Sci.* **2020**, *505*, 144627. [[CrossRef](#)]
40. Liu, W.; Liu, W.; Wei, D.; Li, M.; Zhao, Q.; Xu, S. Synthesis of N,N-Bis(2-Hydroxypropyl)Laurylamine and Its Flotation on Quartz. *Chem. Eng. J.* **2017**, *309*, 63–69. [[CrossRef](#)]
41. Huang, Z.; Zhang, S.; Zhang, F.; Wang, H.; Zhou, J.; Yu, X.; Liu, R.; Cheng, C.; Liu, Z.; Guo, Z.; et al. Evaluation of a Novel Morpholine-Typed Gemini Surfactant as the Collector for the Reverse Flotation Separation of Halite from Carnallite Ore. *J. Mol. Liq.* **2020**, *313*, 113506. [[CrossRef](#)]
42. Filippov, L.O.; Severov, V.V.; Filippova, I.V. An Overview of the Beneficiation of Iron Ores via Reverse Cationic Flotation. *Int. J. Miner. Process.* **2014**, *127*, 62–69. [[CrossRef](#)]
43. Duan, H.; Liu, W.; Wang, X.; Liu, W.; Zhang, X. Effect of Secondary Amino on the Adsorption of N-Dodecylethylenediamine on Quartz Surface: A Molecular Dynamics Study. *Powder Technol.* **2019**, *351*, 46–53. [[CrossRef](#)]
44. Ren, L.; Qiu, H.; Zhang, Y.; Nguyen, A.V.; Zhang, M.; Wei, P.; Long, Q. Effects of Alkyl Ether Amine and Calcium Ions on Fine Quartz Flotation and Its Guidance for Upgrading Vanadium from Stone Coal. *Powder Technol.* **2018**, *338*, 180–189. [[CrossRef](#)]
45. Zhang, H.; Chai, W.; Cao, Y. Flotation Separation of Quartz from Gypsum Using Benzyl Quaternary Ammonium Salt as Collector. *Appl. Surf. Sci.* **2022**, *576*, 151834. [[CrossRef](#)]
46. Liu, W.; Liu, W.; Zhao, Q.; Peng, X.; Wang, B.; Zhou, S.; Zhao, L. Investigating the Performance of a Novel Polyamine Derivative for Separation of Quartz and Hematite Based on Theoretical Prediction and Experiment. *Sep. Purif. Technol.* **2020**, *237*, 116370. [[CrossRef](#)]

Disclaimer/Publisher’s Note: The statements, opinions and data contained in all publications are solely those of the individual author(s) and contributor(s) and not of MDPI and/or the editor(s). MDPI and/or the editor(s) disclaim responsibility for any injury to people or property resulting from any ideas, methods, instructions or products referred to in the content.